Death of embryos from 2300-year-old quinoa seeds found in an archaeological site

Hernán Pablo Burrieza [a], Agustín Sanguinetti [a], Catalina Teresa Michieli [b], Héctor Daniel Bertero [c], Sara Maldonado [a],*

[a] *Instituto de Biodiversidad y Biología Experimental y Aplicada, Consejo Nacional de Investigaciones Científicas y Tecnológicos (IBBEA-CONICET), Argentina*
[b] *Instituto de Investigaciones Arqueológicas y Museo Prof. Mariano Gambier, Facultad de Filosofía, Humanidades y Artes, Universidad Nacional de San Juan, Argentina*
[c] *Cátedra de Producción Vegetal, Facultad de Agronomía, Universidad de Buenos Aires, Argentina*

A B S T R A C T

In the 1970s, during excavations at Los Morrillos, San Juan, Argentina, quinoa seeds were found within ancient pumpkin crocks protected from the light and high temperatures, and preserved in the very dry conditions of the region. The radiocarbon dates confirmed the age of these seeds at around 2300 years. Sectioning of some of these seeds showed reddish-brown embryos, different from the white embryos of recently harvested quinoa seeds. The ancient seeds did not germinate. The structure of the embryo cells was examined using light and transmission electron microscopy; proteins were analyzed by electrophoresis followed by Coomassie blue and periodic acid Schiff staining and fatty acids by gas chromatography. The state of nuclear DNA was investigated by TUNEL assay, DAPI staining, ladder agarose electrophoresis and flow cytometry. Results suggest that, although the embryo tissues contained very low water content, death occurred by a cell death program in which heterochromatin density was dramatically reduced, total DNA was degraded into small fragments of less than 500 bp, and some proteins were modified by non-enzymatic glycation, generating Maillard products. Polyunsaturated fatty acids decreased and became fragmented, which could be attributable to the extensive oxidation of the most sensitive species (linolenic and linoleic acids) and associated with a collapse of lipid bodies.

© 2016 Elsevier Ireland Ltd. All rights reserved.

1. Introduction

Quinoa (*Chenopodium quinoa* Willd.) is a pseudo-cereal that has been grown in the Americas, especially along the Andes, for over 5000 years. The species has numerous genotypes, which are well adapted to extreme environmental conditions with regards to altitude, soil salinity, amount of annual precipitation and minimum temperatures [1,2]. The species is valuable because of the exceptional balance of amino acids in its proteins and nutritionally favorable lipids stored in the tissues of its embryos as well as due to the starch stored in its perisperm [3].

In this study, we analyzed archaeological seeds of quinoa found during an excavation at Los Morrillos, San Juan, Argentina, site iden-tified as Gruta 1, BF, 40–50 [4–6]. In the cave, seeds were found stored within ancient pumpkin crocks protected from light, humidity and high temperature. In this region, the weather is mostly desert-like with little rainfall and marked temperature ranges, with remarkable differences in temperature between night and day as well as between summer and winter, with a significant solar radiation [4–6]. Here, we compared these ancient seeds with quinoa seeds of two currently cultivated genotypes: Utusaya and PRJ. These genotypes were selected as controls because they are usually grown in highly contrasting environments and thus were expected to have constitutive differences in the characteristics of their seeds (probably covering a wide range of variations). The genotype Utusaya is found in the Bolivian Altiplano, at 3600–4000 m altitude, and is adapted to the very arid conditions characteristic of the Altiplano, with less than 250 mm of annual rain and a minimum temperature of $-1\,^\circ$C; the genotype PRJ grows at sea level in the southern region of central Chile, and is adapted to more humid conditions (800 to 1500 mm of annual rain), and temperatures above $5\,^\circ$C.

An orthodox seed usually exhibits its maximum germination potential soon after harvest, and as storage time increases, it loses

* Corresponding author at: Facultad de Ciencias Exactas y Naturales, Universidad de Buenos Aires, Intendente Güiraldes2160 (C1428EGA), Ciudad Autónoma de Buenos Aires, Argentina.
E-mail addresses: saram@bg.fcen.uba.ar, saram.maldonado@gmail.com (S. Maldonado).

vigor and finally dies. The rate of physiological ageing generally increases with increased moisture content and temperature. The ability of an orthodox seed [7] to survive at very low intracellular water content is the basis for its longevity, maintaining viable embryos over centuries [8] or even millennia [9–11]. However, there are no studies about the type of cell death in tissues of orthodox seeds preserved under gene banks conditions, whose embryos are constituted by storage tissue i.e. cells with de-differentiated organelles, absence of vacuoles, and consequently very low water content, with protein and lipid bodies occupying most of the cellular lumen. It is known that embryos of orthodox seeds always maintain a certain low level of metabolic activity, which varies depending on the longevity of the seed [12,13]. Low metabolism delays ageing but does not prevent seeds from eventually dying. According to Kranner et al. [14], the mechanisms underlying seed ageing and death are less understood than seed longevity as a function of water content and temperature.

The two modes of plant cell death, programmed cell death (PCD) and necrosis, differ fundamentally in their morphology, biochemistry and biological relevance [15]. Accurate identification of the mode of cell death occurring in a particular situation is a necessary prerequisite to understand the biological process taking place, specifically differences between PCD and necrosis during storage. PCD consists of an ordered sequence of cellular events, which includes the transcription of specific genomic sequences, synthesis of specific proteases, and activation of nucleases. Extensive literature exists regarding the associated molecular, biochemical and morphological changes involved [16–23].

Kranner et al. (2011) reported internucleosomal DNA fragmentation during pea seed ageing and suggested that artificial ageing induces a complex process of interlinked programmed and non-programmed events, which lead to cell death. Anyway, the DNA laddering found in aged and dead pea seeds suggests that degradative processes during seed ageing at 12% water content involve enzymatic activity, including that of caspase-like proteins involved in cell death during dry ageing [14]. Likewise, it is well established that enzymatic and nonenzymatic products of polyunsaturated fatty acid oxidation are implicated in essential aspects of cellular aspects of cellular signaling, including the induction of PCD [24–26]. Glycation also has a fundamental role in many processes leading to cell death; glycans, either alone or complexed with glycan-binding proteins, can deliver intracellular signals or control extracellular processes, which induce the initiation and execution of cell death programs [25]. On the other hand, necrosis is typically an acute cell death response that develops rapidly, but is no longer considered an unprogrammed process [15]. At this time, necrosis remains poorly characterized at the biochemical and genetic levels, so there are as yet no molecular markers of necrosis [15,26,27].

Archaeological seeds degrade into small fragments over thousands of years, and the PCR product size decreases to less than 300 bp [28]. Different authors [29,30] have reported that the DNA from charred seeds is often of higher weight than that from specimens that are morphologically well-preserved, i.e. seeds die within a slow process of PCD. Then, DNA yield and molecular weight are dependent on the initial condition of the sample and storage conditions that prevent nuclease activity.

We have previously hypothesized that quinoa seeds, an orthodox seed [31–34] under the conditions of preservation of the cave where they were found, could have maintained their viability for a long time. If they finally died, then, it might be interesting to find out what kind of death occurred in the cells of embryo tissues of an orthodox seed, which lack vacuoles [3].

In the present study, we examined the embryo tissues of the ancient quinoa seeds found at Los Morrillos and embryos of two existing quinoa genotypes (PRJ and Utusaya), using a range of well-established markers of PCD such as: (i) morphological changes in nuclei, mitochondria, plastids, and storage reserves (lipid and protein bodies), (ii) DNA degradation, (iii) lipid oxidation, and (iv) protein degradation. The structure of the embryo cells was studied using light and transmission electron microscopy (TEM) and proteins were analyzed by electrophoresis followed by Coomassie blue and periodic acid Schiff (PAS) staining; fatty acid oxidation was studied by gas chromatography: the state of nuclear DNA was investigated by terminal deoxynucleotidyltransferase-mediated dUTP-biotin nick end labeling (TUNEL), DNA ladder and flow cytometry. Then, we discussed about the type of death that occurred in the embryos of these ancient seeds and finally concluded that it is a non-vacuolar type of PCD, so far not described in the literature.

2. Material and methods

2.1. Material

Archaeological quinoa seeds were gathered at a burial site from the Ansilta civilization located in an Andean cave in Los Morrillos, San Juan, Argentina from Los Morrillos, Gruta 1, BF, 40–50 [4–6]; (Fig. 1). The seeds (approximately 2.5 kg) were found within ancient pumpkin crocks protected from the light and high temperatures, and preserved in the very dry conditions of the region (annual rainfall ranging from 20 to120 mm; rains occur more often during the summer). Average temperatures range from 10 °C to 35 °C. The site is at 31°42′, 46.58′í south and 69°44′13.28′í west, at an altitude of 2935 m above sea level [4,5].

Likewise, seeds of two existing quinoa genotypes, Utusaya and PRJ, were analyzed as controls (Fig. 1A). The seeds of genotype PRJ were provided by the Bank of Germplasm INIA-Vicuña, Chile, whereas the seeds from genotype Utusaya were provided by the Bank of Germplasm, Universidad Mayor de San Andrés, La Paz, Bolivia.

2.2. Calculation of radiocarbon dates

The radiocarbon dates were measured by beta counting and Accelerator Mass Spectrometry (AMS). Beta counters measure the radioactivity of the sample, whereas AMS determines the ratio of the three different carbon isotopes in the sample.

2.3. Viability as determined by the 2,3,5-Triphenyl-2H-Tetrazolium chloride (TTC) test and confirmed by fluorescein diacetate staining

Seeds were soaked in water overnight, and then placed in a 0.1% tetrazolium chloride solution (2,3,5 triphyenyl tetrazolium chloride in water) for 3 h at 30 °C, according to the recommendation of The International Seed Testing Association (Supplements 2011 to ISTA Working Sheets on Tetrazolium Testing, Volume I and II).

Viability was also determined by Fluorescein Diacetate (FDA: Sigma-Aldrich Co. LLC, C-7521). The FDA stock solution was prepared by dissolving 5 mg of FDA in 1 ml acetone and solution was stored at −20 °C. Fresh sections were obtained with a razor blade and mounted on slides. Following addition of staining solution (50 μmol), sections were incubated at room temperature for 5 min in the dark. After that, the staining solution was removed with PBS and then analyzed with fluorescent microscopy. A FDA filter set (excitation 488 nm, emission 530 nm) was used to examine the samples.

2.4. Germination and humidification treatment (priming)

Seeds of the three genotypes were tested for germination on top of three pieces of filter paper moistened with 3.5 cm³ distilled-
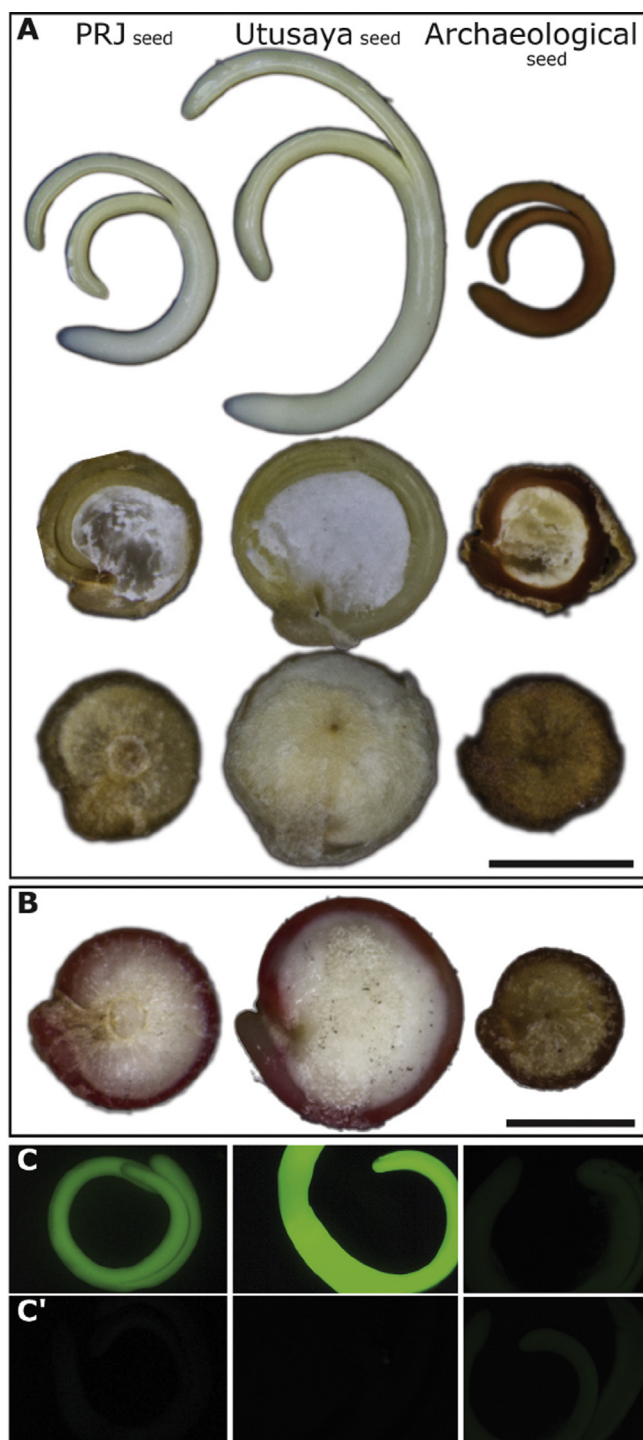
Fig. 1. Panel A. Embryos, seeds and fruits from PRJ (left), Utusaya (center) and archaeological (right) seeds. Bar: 2 mm. Panel B. PRJ (left), Utusaya (center) and archaeological (right) seeds after tetrazolium treatment. Bar: 2 mm. Panel C and Cí. PRJ (left), Utusaya (center) and archaeological (right) seeds after FDA treatmentí: C, treated seeds; Cí. Controls. Bar: 2 mm.

deionized water in 6-cm-diameter Petri dishes at 25 °C ± 1 °C and 16 h fluorescent light/8 h dark for 6 days. Three replicates of 50 seeds were used for each genotype.

The effect of priming on the germination of archaeological seeds was tested. Three seed lots were used for each genotype. Seeds were maintained in a saturated atmosphere (100% relative humidity), at 25 °C.

2.5. Sample preparation for light microscopy and transmission electron microscopy (TEM)

For histological analysis, and TUNEL assays, quinoa seeds and isolated embryos (Fig. 1) were fixed for 4 h at 4 °C in 4% paraformaldehyde with 0.1 M phosphate buffered saline (PBS) (pH 7.2), dehydrated in a graded ethanol series (30%, 50%, 70%, 90%, 100%) and embedded in LRW resin (Polyscience Inc., Warrington, PA, USA; 17411) as previously described [35]. Semi-thin sections (1 μm thick) were mounted on glass slides, and either stained with 0.5% toluidine blue O (Sigma-Aldrich, St. Louis, MO, USA) in aqueous solution or used without staining.

For subcellular analysis, small embryo fragments (1 mm^3) were fixed for 2 h at 4 °C using 2.5% glutaraldehyde in 0.1 M PBS, pH 7.2. They were post-fixed later in 1% OsO_4 in the same buffer for 60 min, dehydrated in a graded ethanol series followed by an ethanol-acetone series and embedded in Spurr's resin (Sigma-Aldrich). Ultrathin sections were obtained with an ultramicrotome (Reichert-Jung, Vienna, Austria) using a diamond knife, mounted on grids coated with Formvar (Polyscience Inc.), stained in uranyl acetate followed by lead citrate (EMS, Hatfield, PA, USA), and examined in a Zeiss M109 turbo (Zeiss, Wiesbaden, Germany) transmission electron microscope operating at an accelerating voltage of 90 kV.

2.6. DNA isolation and analysis

Genomic DNA was isolated from 50 mg seeds of the three genotypes (PRJ, Utusaya and archaeological seeds) using the DNeasy plant mini kit (Qiagen, Germany). Yield and quality of the DNA obtained were assessed in a NanoDrop spectrophotometer (Thermo Scientific NanoDrop 2000c). A 1.5-μg aliquot of DNA was separated from each genotype on a 0.8% (w/v) agarose gel, and stained with ethidium bromide (final concentration: 0.5 μg/ml). A 1-kb DNA ladder (Genbiotech, Buenos Aires, Argentina) was used as a reference.

2.7. Flow cytometry analysis

Embryos were dissected and chopped with Otto I extraction buffer and the nuclei-containing suspension was passed through a 50-μm filter. Then, nuclei were stained with two volumes of Otto II staining solution containing propidium iodide [36,37]. After gently shaking the solution, samples were analyzed with a flow cytometer (CyFlowPloidyAnalyser, Partec). Single-parameter histograms displayed a single measurement parameter (relative fluorescence) on the x-axis and the number of events (cell count) on the y-axis.

2.8. TUNEL assay

DNA fragmentation was detected by TUNEL using the *in situ* Cell Death Detection Kit, Rhodamine (Roche). Cross sections were obtained as described above. TUNEL was performed according to the manufacturerís instructions. Briefly, sections were permeabilized with 20 μg ml−1 proteinase K for 20 min at room temperature and washed four times with PBS. The labeling reaction was performed at 37 °C in a dark, humid chamber for 1 h. A negative control was included in each experiment by omitting Terminal deoxynucleotideTransferase (TdT) from the reaction mixture. As a positive control, permeabilized sections were incubated with DNase I (3U/ml) for 15 min before the TUNEL assay. The sections were mounted using Citifluor^{TM} mounting medium (EMS).

Control treatments were conducted for each set of slides. TUNEL was absent when TdT was omitted (data not shown). In positive controls previously treated with DNase, all nuclei were labeled, thus validating the procedure.

Images for histological analysis and TUNEL were obtained by light microscopy and epifluorescence with an Axioskope 2 microscope (Carl Zeiss, Jena, Germany). A rhodamine filter (excitation/emission: 577/590) was used to examine the samples. Images were captured with a Canon EOS 1000 D camera (Tokyo, Japan) and analyzed using the AxioVision 4.8.2 software package (Carl Zeiss). Counterstaining was done with 0.02 mg ml^{-1} 4′,6-diamidino-2-phenylindole (DAPI) staining [22]. A DAPI filter (excitation 340–390 nm, emission 420–470 nm) was used to examine the samples. Images were captured with a Canon EOS 1000 D camera (Tokyo, Japan) and analyzed using the AxioVision 4.8.2 software package (Carl Zeiss).

2.9. Protein analysis

Seeds (500 mg dry weight) were ground to a powder. The flour was diluted in 1 ml miliQ water. The homogenate was incubated for 1 h at 4 °C. The extracts were centrifuged for 10 min at 12,000g, at 4 °C, and the supernatant was collected to eliminate tissue debris (Fraction 1). This step was repeated and the pellet was suspended in NaCl 0.5 M, incubated for 1 h at 4 °C, and centrifuged; the supernatant was then collected (Fraction 2). The pellet was next suspended in 0.3 N NaOH, incubated for 1 h at 4 °C, and centrifuged at 12,000g; the supernatant was collected (Fraction 3). The pellet was suspended in a buffer containing 50 mM Tris-HCl pH 6.8, 2% SDS, 0.5% beta-mercaptoethanol and 8 M Urea, and then incubated for 1 h at 4 °C, and centrifuged at 12,000g; the supernatant was collected (Fraction 4).

Fractions 1 to 4 were precipitated with 22.5% TCA (trichloroacetic acid), 1 ml + 750 TCA (50%) for 48 h at 4 °C. The samples were first centrifuged at maximum speed at 4 °C for 10 min; the supernatant was discarded. Subsequently, the pellet was rinsed four times with cold acetone and left to dry at 4 °C overnight. The proteins were resuspended in 250 μl of a 50 mM Tris-HCl buffer pH 6.8 containing 2% SDS, 0.5% beta-mercaptoethanol and 8 M Urea and incubated overnight. Then, the extracts were electrophoresed, and 15 μl of each fraction was sown on an SDS-polyacrylamide gel 12.5% (SDS-PAGE, Bio-Rad system) and stained with Coomassie brilliant blue. For glycoprotein detections, gels were stained using the periodic acid-Schiff reagent [38]. A PageRuler^{TM} Prestained Protein Ladder, 10 to 180 kDa (Fermentas, USA) was used as molecular mass standard.

2.10. Fatty acid analysis

The Bligh & Dyer method [39] with minor modifications was used to extract the lipid fraction from quinoa seeds for fatty acid analysis. Quinoa seeds (2 g) were milled in an ULTRA-TURRAX Tube Drive system (IKA, Staufen, Germany) with stainless steels balls at 6000 rpm for 3 min to obtain fine flour. After that, 5.7 ml of methanol, 2 ml of ultrapure water and 2.35 ml of chloroform were added. The mixture was homogenized for 2 min, and 3 ml of ultrapure water and 3.6 ml of chloroform were added and homogenized for 2 min. The mixture was transferred to a separate funnel. The bottom phase containing oil in chloroform was separated and desorbed by solvent evaporation under nitrogen flow at 40 °C until constant weight. The extracted oil was stored at −18 °C under a nitrogen atmosphere in sealed vials.

Fatty acid composition was determined by gas chromatography after derivatization of extracted oils to fatty acid methyl esters (FAME) according to the AOAC Official Method 19TH EDITION, 2012. An Agilent 6850 gas chromatography system (Agilent, Santa Clara, CA, USA) with a split injector, a fused silica capillary column coated with poly (biscyano) propyl siloxane (60 m in length, 0.25 mm i.d., 0.20 lm film thickness, SP-2340 Supelco) and a flame ionization detector was used. Helium was used as a carrier gas at a flow rate of 0.6 ml/min. The injector temperature was 260 °C. The initial oven temperature was held at 140 °C for 5 min and then a temperature gradient from 140 °C to 240 °C at 4 °C/min was applied. Identification of FAME was based on the retention time of standard esters (Supelco 37-component FAME Mix, Bellefonte, PA, USA). Peaks were integrated using the ChemStation software (Santa Clara, CA. USA). Assuming that the content of FAME was close to the sample weight (100%), the fatty acid profiles were expressed as a methyl ester percentage of the total area of the chromatogram.

3. Results

3.1. Age, viability and germination ability of seeds

The radiocarbon dates, as measured by beta counting and AMS, were Beta–147321 = 2300 ± 60 BP.

The TTC test was used to prove seed viability (Fig. 1B). After the TTC treatment, both PRJ and Utusaya white embryos produced a normal red color, demonstrating dehydrogenase activity. The brown embryos of the archaeological seeds did not become stained, maintaining the original brown color, which indicated that these enzymes had been denatured or degraded.

Fluorescein diacetate (FDA) was also used to prove seed viability (Fig. 1C–Cí). FDA is a cell-permeant esterase substrate, which can serve as a viability test that measures both enzymatic activity, which is required to activate its fluorescence, and cell-membrane integrity, which is required for intracellular retention of their fluorescent product. After the FDA treatment, both PRJ and Uusaya embryo tissues exhibited yellowish green fluorescence, proving esterase activity (Fig. 1C). Conversely, the embryos of the archaeological seeds did not become fluorescent (Fig. 1C).

Both control genotypes showed 70.4% ± 4.78 and 88.17 ± 4.85 (means ± SD) total germination, respectively. In contrast, the ancient seeds did not germinate, even when subjected to priming.

3.2. The TEM (transmission electron microscopy) study revealed the severity of the cellular damage

The embryos of the control seeds exhibited the characteristics of the embryo tissues previously described for other quinoa genotypes [3]: the cell lumen was almost fully occupied by protein and lipid bodies and the cytoplasm was a network around them (Fig. 2 panel A). Protein bodies contained one or more globoids in their protein matrix; also, they often showed empty areas, which had been previously occupied by the globoid crystals before they were dissolved during fixation (because the fixation procedure may extract phytates), or chipped out during sectioning. Plastids and mitochondria were dedifferentiated (Fig. 2e–h). The nuclei displayed heterochromatin and the nucleolus stained strongly (Fig. 2 i); no plasmolysis or exocytosis was detected (Fig. 2a–d,i).

The embryo tissues of ancient seeds, as analyzed by light microscopy, did not seem very different from the controls (Fig. 2j–l). In fact, protein and lipid bodies and nuclei with nucleoli were all detected in the different tissues of the archaeological embryos (Fig. 2j–l). The protein bodies looked compact and remained visually unaltered, containing the empty areas corresponding to the crystal globoids (Fig. 2 j-l). However, the TEM analysis revealed key differences that were not visible by light microscopy, as follows: (i). Cells were plasmolyzed and cell walls were strongly degraded (Fig. 2, panel B j-n, asterisk). (ii). Lipid bodies collapsed (Fig. 2 m-r). (iii). The stroma of mitochondria and chloroplasts stained strongly and, consequently, neither phytoferritin of proplastids nor cristae of mitochondria were detected; only the size (smaller) of mitochondria remained the same, which allowed identifying them (Fig. 2p–q). (iv). Nuclei preserved their lobed form, but lobes were
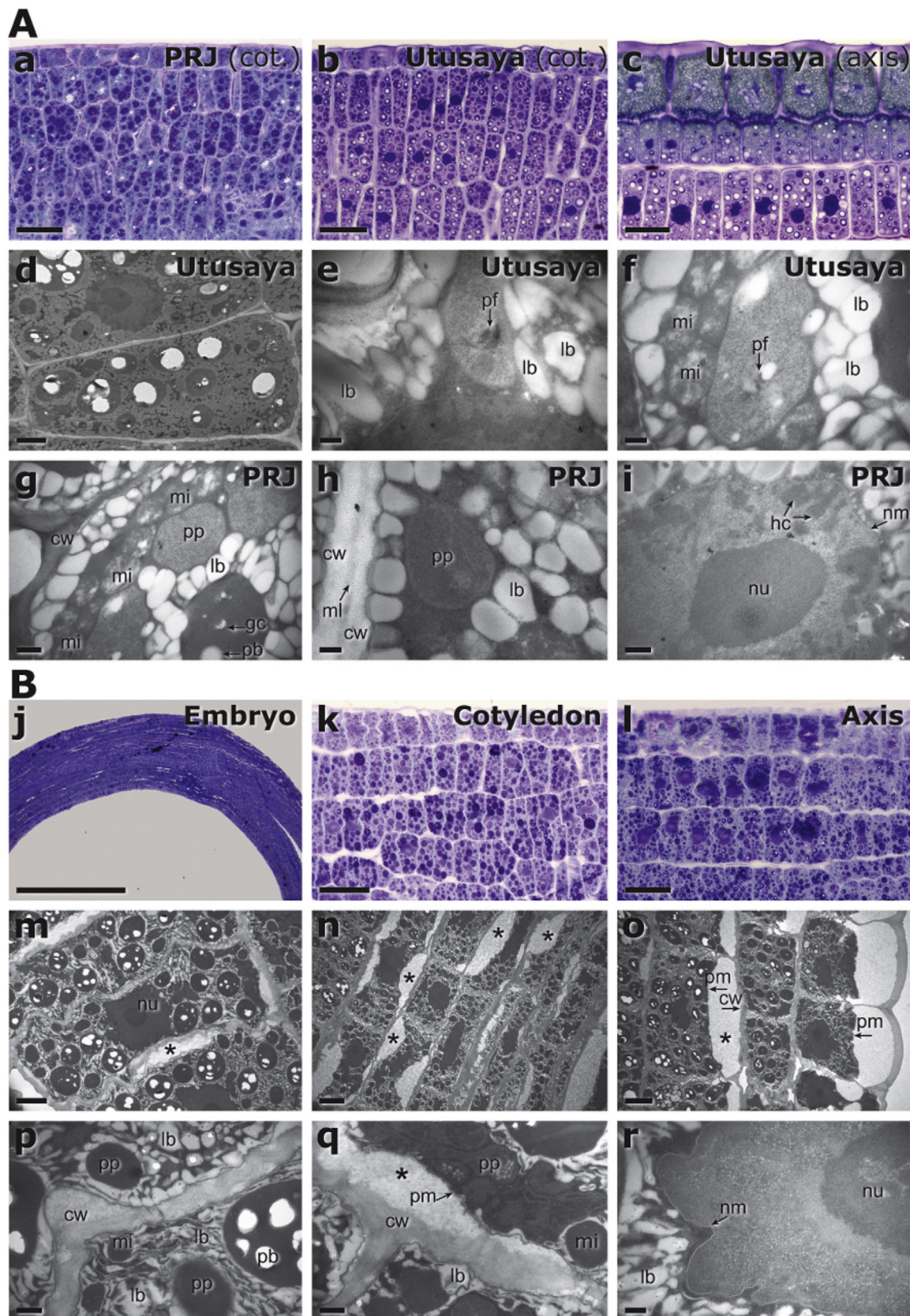
Fig. 2. Panel A. Light microscopy (LM) micrographs: (a). Median section of PRJ cotyledon. (b) Utusaya cotyledon. (c) Utusaya axis. (d–f) Transmission electron microscopic (TEM) micrographs of sections of Utusaya and (g–i) PRJ embryo tissues. (d–f) Section of ground meristem, and (g–i) leaf spongy tissue. Protein bodies (pb) of figures d and g contained globoid crystals (gc) or empty areas, which contained globoid crystals before they were dissolved during fixation or chipped out during sectioning. In figures e–h, proplastids (pp) contained clusters of particles of phytoferritin (pf) and some vacuole-like structure. In figures e–i, lipid bodies (lb) can be seen turgid, polygonal and circular in shape. In d and i, the nucleus with nucleolus (nu), nuclear membrane (nm), and chromatin (ch) can be observed. In figures f–g, several mitochondria (mi) are grouped. Cells are not plasmolyzed, and cell walls (cw) are compact and the middle lamella is always observed. Bars: a–c: 20 μm; d. 2 μm; e,-f: 100 nm; g-i: 200 nm.

marked more deeply (Fig. 2q). Also, nuclei conserved the nuclear membrane and nucleolus, but heterochromatin was not detectable (Fig. 2r).

3.3. In archaeological seeds, DNA degraded into small fragments

DNA integrity was evaluated by agarose gel electrophoresis, TUNEL assays, and flow cytometry (Fig. 3). In control seeds, the extracted DNA produced one well-bound band of high-molecular weight, without traces of fragmentation (Fig. 3, Panel A). As opposed to control seeds, the DNA extracted from the dead ancient seeds formed a thick band with diffuse edges, and molecular weight below 540 bp. The presence of this band, which is formed by the migrating fragments of low molecular weight, is a clear demonstration of cell death and an endpoint of nuclear DNA degradation (Fig. 3, Panel A).

In nuclei of archaeological embryos, the fluorescein-dUTP-labeling assay did not detect nuclear DNA cleavage (Fig. 3, panel B). The absence of reaction in the nuclei of archaeological embryos and their positive control can be attributable to the strong DNA fragmentation. On the other hand, the TUNEL assay did not detect fluorescence in the nuclei of PRJ and Utusaya embryos (Fig. 3, panel B), but did so in their respective positive controls, staining the nuclei of all cells. In the ancient seeds, DAPI staining confirmed the absence of DNA with high molecular weight as well as the state of deterioration of the residual DNA; in fact, while the nuclei of Utusaya and PRJ embryos exhibited strong fluorescence, the nuclei of the archaeological embryos showed no fluorescence.

In control seed embryos (Utusaya and PRJ genotypes), flow cytometry revealed two clear peaks, which were related to 2C and 4C values: 2C indicates the DNA level corresponding to the diploid state of the genome (G_1 phase of the cell cycle), whereas 4C indicates the ability of cells to enter the M stage of the cell cycle (i.e. G_2 phase of the cell cycle) (Fig. 3, Panel C).

In ancient seed, dead embryo cells produced a broad area formed by very low peaks which could be related to 4C, 2C and sub-G_1 values (Fig. 3, Panel C). The presence of sub-diploid peaks in the DNA fluorescence histogram is a specific marker of DNA degradation [40].

TEM analysis, agarose gel electrophoresis, TUNEL, DAPI, ladder assays, and flow cytometry, each by itself but also complementarily, conclusively confirmed the occurrence of a program of cell death which occurred at some time within the long time elapsed.

3.4. During the storage time, some proteins were modified by non-enzymatic glycation

The different protein fractions of the major storage proteins were sequentially extracted from the archaeological seeds and the control genotypes PRJ and Utusaya. The procedure was based on water (fraction 1), saline (fraction 2), and alkaline (fraction 3) solubility. In addition, a fraction was obtained using a strong denaturant and reducing buffer containing SDS, beta-mercaptoethanol and urea (fraction 4). It should be noted that water is the best buffer to solubilize albumins while high salt concentrations favor the extraction of globulins. The compositions of the resulting four protein fractions were analyzed by SDS-PAGE and stained with Coomassie brilliant blue to detect proteins (Fig. 4A) and PAS reagent to reveal protein glycation (Fig. 4B).

As shown in control seeds (Fig. 4A, lanes 1 and 2), the proteins were resolved into distinct bands that spanned a broad range of molecular weights from 10 kDa to > 100 kDa. Both controls showed major bands of: (i) 58, 36, 34, 31, 24 kDa (water-soluble proteins); (ii) 58, 40, 38, 36, 31, 20, 18, and 14–13 kDa (high salinity-soluble proteins) and (iii) 73, 66, 34, 20, 18 kDa (denaturant and reducing buffer-soluble proteins). Some differences in the band patterns between the genotypes used as controls were evident: genotype Utusaya showed a band of 38 kDa, whereas genotype PRJ showed two bands of 40 and 36 kDa. The highest protein bands, here detected in both controls, would correspond to albumin fractions followed by globulins, which were obtained in fraction 2 and (traces) fraction 4. Globulins are characterized by having two heterogeneous sets of polypeptides in the size ranges: 30–40 kDa and 20–25 kDa, which are joined by disulfide bonds in the native protein [41]. Polypeptides in the 30–40 kDa and 20–25 kDa size ranges (obtained mostly from the saline-soluble fraction) would correspond to different isoforms of the 11S globulin, called chenopodin, which were previously described in embryos of *C. quinoa* by Brinegar and Goundan [42]. Likewise, the globulins of 36, 38 and 40 kDa above-mentioned had been previously reported by Fairbanks et al. [43] as very variable within and among different quinoa accessions.

Some bands of globulins in the saline-soluble fraction were revealed as glycated when gels were stained with the PAS reagent (Fig. 4B). Compared to controls, the corresponding profile of the archaeological seed proteins (Fig. 4A–B, lane 3) revealed substantial differences, which can be summarized as follows:(i) No bands were detected in water- and saline-soluble fractions. (ii) A general reaction with barely defined bands (35, 22 and 18 kDa) was detected weakly in alkaline-soluble fraction and strongly in the denaturant and reducing buffer-soluble fraction (fractions 3 and 4, respectively). (iii) A thick deposit of material of very high molecular weight, consistent with non-specific cleavage, and protein crosslinking, characteristic of non-enzymatic glycation, were observed at the boundary between the stacking and resolving gels in the lanes where the denaturant and reducing buffer fractions had been loaded and the gel stained with Coomassie blue (fraction 4). When the gel was stained with the PAS reagent to detect glycosylated proteins, denaturant and reducing buffer-soluble fraction, and also the water- and alkaline-soluble fractions showed that these deposits were mainly composed of glycosylated proteins (Fig. 4B). Then, the glycation that had occurred in the storage proteins of archaeological embryos can be associated with the Maillard reaction, which did not alter the morphology of the protein bodies (Fig. 2j–p) but caused browning of embryonic tissues (Fig. 1).

3.5. Unsaturated fatty acids decreased or became fragmented by oxidation

The fatty acid composition of the archaeological seeds and of the control genotypes PRJ and Utusaya was determined by gas chromatography after derivatization of extracted oils to FAME. The profiles of polyunsaturated fatty acids of the archeological seeds and controls showed significant differences (Table 1), caused by oxidation of the most sensitive fatty acid species (C18: 3, linolenic and C18: 2, linoleic). The main differences detected were: (i) decrease in the relative percentage of polyunsaturated fatty acids; (ii) relative increase in the percentage of the fractions of saturated fatty acids; and (iii) presence of the signal (only detected in the archaeological seeds) corresponding to caproic acid (C6:0), con-

Panel B. (j–l). LM micrograph of an archaeological embryo. (j) Embryo median section; (k) Cotyledon section. (l) Axis section. (m–r). TEM micrographs of sections of archaeological embryo tissues. (m–o). (m) Ground meristem. (n) Procambium. (o) Protodermal and spongy tissues of cotyledon. (p), Subcellular details of m. (q–r) Subcellular details of o. Details show plasmalemma (pm) partially separated from cell walls (cw) and lipid bodies (lb) strongly collapsed; q, mitochondrion (mi) and proplastids (pp) very degraded, **i**. the nucleus with nucleolus (nu) and nuclear membrane (nm), but absence of chromatin. Bars: j: 500 μm; k–l: 50 μm; m–o: 2 μm; p–q: 200 nm; r: 100 nm.
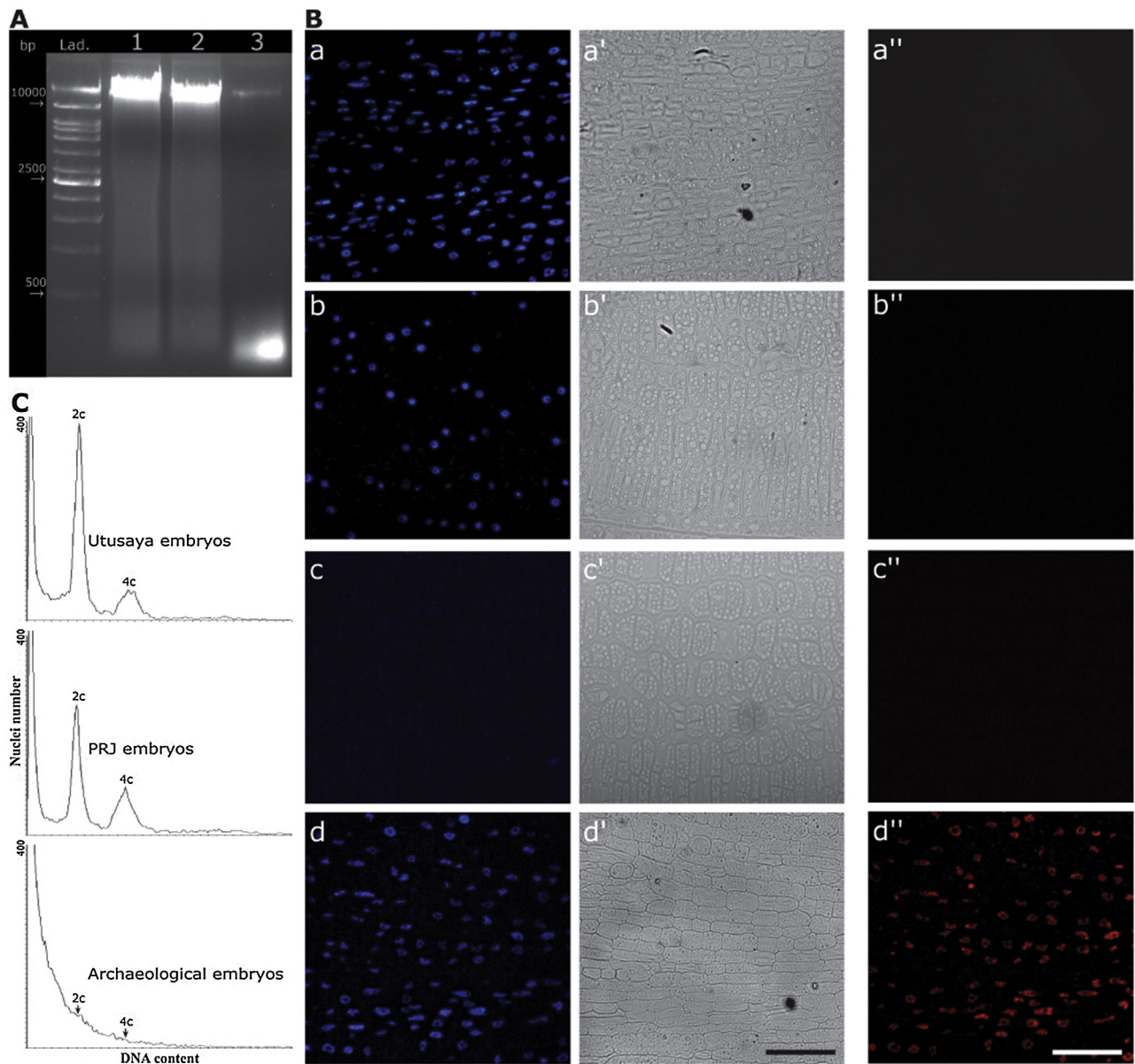
Fig. 3. Panel A. Nucleic acid integrity in embryo tissues as evaluated by agarose gel electrophoresis.PRJ (lane 1), Utusaya (lane 2) and archaeological (lane 3) embryos.
Panel B. TUNEL analysis: Nuclei with fragmented DNA were detected only in the TUNEL-positive controls of control genotypes. In the first column, nuclei are seen by fluorescence (excitation 340–390 nm, emission 420–470 nm) after DAPI staining. In the second column, tissues are seen by phase contrasting. In the third column, tissues are seen by fluorescence (excitation/emission: 577/590) after TUNEL treatment. **a-aíí**. PRJ cotyledons; **b-bíí**. Utusaya cotyledons; **c-cíí**. Archaeological cotyledons; **d-díí**. Positive control in a section of Utusaya cotyledons. Bars: 100 μm.
Panel C. Flow cytometric measurement of mean nuclear ploidy at PCR, Utusaya, and ancient embryos from mature seeds. Histograms show the C-DNA levels. The x-axes are the log of the fluorescence intensity: 2C peak corresponds to the diploid state of genome (G_1 phase of the cell cycle); 4C peak indicates the G_2 phase of the cell cycle. The y-axes represent the cell counts (number of events per channel) in a period of time.

firmed by gas chromatography/mass spectrometry analysis, and attributable to the fragmentation of long-chain fatty acids generated after extensive oxidation.

In this way, these differences detected in the profile of the fatty acids of the archeological embryos correlated with the above-mentioned collapse of the lipid bodies (Fig. 2m–r).

4. Discussion

According to Zazula et al. [44], the oldest independently dated ancient seeds known to have germinated and grown into full plants include an ~2000-year-old date palm (*Phoenix dactylifera* L.) seed

excavated from near the Dead Sea [9] and an ~1300- year-old lotus (*Nelumbo nucifera* Gaertn.) seed from China [10,11]. Data on seed germination of ancient seeds, even after ~30,000 years, either are erroneous (as the case of the Arctic lupine seeds reported by Porsild et al. [45] or need to be independently dated (as the cases of Siberian champion and *Persicaria* [46], all of them permafrost preserved [44]. Here, we report quinoa seeds found at Los Morrillos, San Juan, Argentina, stored within ancient pumpkin crocks protected from light and high temperature. The radiocarbon dates, as measured by beta counting and AMS, confirmed the age of these seeds at 2300 ± 60 years. The percentage of germination, before and after priming treatment, was 0% and seeds proved to be unviable.
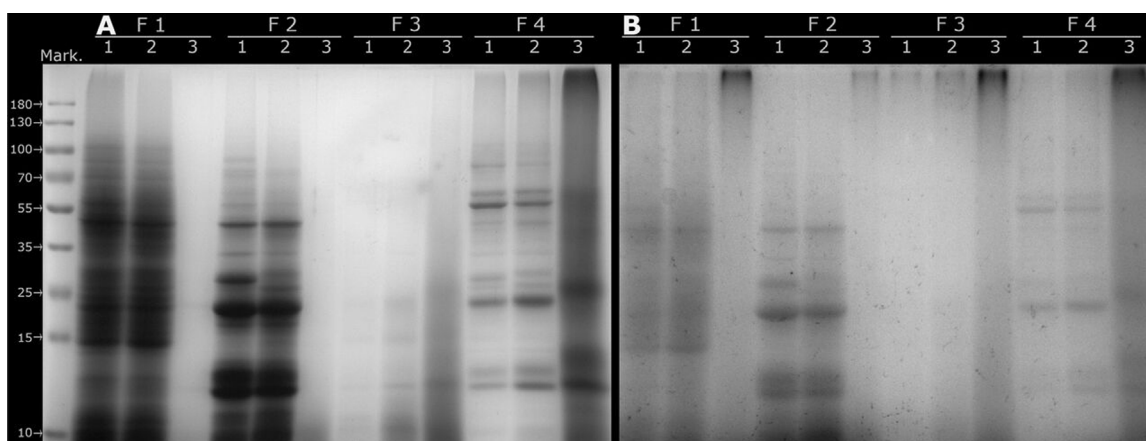
Fig. 4. Sequential SDS–PAGE of quinoa embryo protein fractions: water-, saline-, alkaline- and denaturant and reducing-soluble fractions (fractions 1 to 4, respectively). In all fractions, lanes 1 and 2 correspond, respectively, to genotypes PRJ, and Utusaya, both used as controls; lane 3 corresponds to the archaeological embryos. Gels were stained with: A. Coomassie blue reagent. B. PAS reagent.

Table 1
Fatty acids in Utusaya, PRJ and archeological mature embryos, as determined by gas chromatography after derivatization of extracted oils to fatty acid methyl esters (FAME) according to the AOAC Official Method − 2012.

Fatty acids in quinoa mature embryos of three genotypes (methyl ester percentage of the total area of the chromatogram)				
Lipid name	Fatty acid common names	Utusaya embryos	PRJ embryos	Archaeological embryos
C6:0	Caproic acid	0	0	3.35 ± 0.14
C14:0	Myristic acid	0.12 ± 0.00	0.33 ± 0.01	0.67 ± 0.01
C16:0	Palmitic acid	9.42 ± 0.10	11.15 ± 0.09	34.87 ± 0.15
C16:1	Palmitoleic acid	0.27 ± 0.00	0.22 ± 0.05	0.56 ± 0.02
C18:0	Stearic acid	1.13 ± 0.01	1.00 ± 0.00	3.91 ± 0.04
C18:1	Oleic acid	27.76 ± 0.01	15.07 ± 0.02	37.32 ± 0.10
C18:2	Linoleic acid	43.05 ± 0.08	59.24 ± 0.16	2.94 ± 0.08
C18:3	Alpha-linolenic acid (ALA)	10.38 ± 0.04	7.08 ± 0.01	0
C20:0	Arachidic acid	0.96 ± 0.02	0.87 ± 0.01	4.40 ± 0.10
C20:1	Eicosenoic acid	1.86 ± 0.03	1.24 ± 0.00	3.33 ± 0.03
C22:0	Behenic acid	0.96 ± 0.02	0.87 ± 0.01	4.40 ± 0.06
C22:1	Erucic acid	3.70 ± 0.15	2.80 ± 0.03	3.84 ± 0.05
C24:0	Lignoceric acid	0.46 ± 0.01	0.43 ± 0.01	2.19 ± 0.17

The nucleus is the main target of the cell degradation machinery during PCD. Nuclear degradation processes encompass chromatin events (i.e., chromatin degradation and DNA fragmentation) and nuclear envelope events (i.e., lobbing of the nuclear surface and disassembly of the nuclear pore complex) which occur simultaneously in the same cell [17,47]. There are yet no reports on changes in the storage cells of orthodox seed tissues throughout the years of storage or on the MCP that occurs in these tissues.

According to Gilbert et al. [48,49], the relative rates of various types of DNA damage and their mode of accumulation remain poorly characterized. DNA damage accumulates over time in dead or dormant cells due to factors such as spontaneous hydrolysis and oxidation, and consequently most ancient specimens contain only fragments in the 100–500 bp size range [50–53]. Here, we investigated nuclear degradation by TEM and specifically DNA fragmentation by TUNEL, genomic DNA electrophoresis and flow cytometry.

Results were as follows: (i) the analysis by TEM demonstrated that nuclei had retained their shape and size, preserved the nuclear membrane and the nucleolus, but also that heterochromatin density had been dramatically reduced; the cell death program was different from the autolytic process occurring during the development of water-vacuolated cells of cowpea seed coats, in which nuclear membranes lose their viability and oligonucleosomes accumulate in the cytoplasm [54]; (ii) nuclei showed TUNEL-negative labeling in all embryonic cells, which we interpreted as representing the high damage that affects the DNA molecule;(iii) a thick band with diffuse edges, with molecular weight lower than 540 bp, was evident in the electrophoretic run; and (iv) the flow cytometric study did not detect remarkable peaks but identified a general noise and within it, small peaks which corresponded to the 2C and 4C control embryos values, and also identified several other small sub-G_1 peaks.

Concerning the latter point, DNA replication is discontinuous during the cell cycle [55] and thus lays the basis for subdivision of the cell cycle into four major phases: presynthetic interphase or gap 1 (G_1 phase), DNA synthesis phase (S phase), post-synthetic interphase or gap 2 preceding mitosis (G_2 phase), and mitosis (M phase). All these phases can be identified by a distinct nuclear DNA content of the cells. During the S phase, chromosomal DNA is doubled and therefore cells are characterized by a gradual increase in DNA content from the basic value, which is referred to as the 2C level, to the 4C level [55]. During the M phase, when sister chromatids separate in anaphase, the DNA content drops to the 2C level in the two newly formed daughter cells. In this study, we identified a clear difference between the histograms of control embryos (PRJ and Utusaya) and those of embryos of the ancient seeds. Two peaks (2C and 4C) were clearly detected in control embryos, which correspond, respectively, to the G_1 and G_2 stages of the mitotic cycle [56]. In archaeological embryos the histogram coincides with

others obtained during apoptosis in other systems [40,57]. According to Nicoletti et al. [40], the presence of cells with DNA stain ability lower than that of G_1-cells (sub-G_1 peaks) is considered a marker of cell death by PCD. In animal cells, the appearance of a sub-diploid DNA peak is a specific marker of apoptosis; necrosis induced by metabolic poisons or lysis produced by complement does not induce any sub-G_1 peak in the DNA fluorescence histogram; the sub-G_1 peak can also represent mechanically damaged cells, cells with reduced chromosome number (aneuploid cells) and isolated apoptotic bodies. The reduced stainability of apoptotic cells is the direct consequence of partial DNA loss due to the activation of endogenous nucleases and diffusion of low-molecular weight DNA (as oligonucleosomes and mononucleosomes) outside the cells.

As opposed to control seeds, the DNA extracted from the dead ancient seeds formed a thick band with diffuse edges and a molecular weight below 540 bp. The presence of this band, which is formed by the migrating fragments of low molecular weight, is a clear demonstration of cell death and an endpoint of nuclear DNA degradation (Fig. 3, Panel A).Further studies are required to obtain more information about this response, specifically in the probable oxidation of a high proportion of cytosine and thymine bases in DNA over time after the death. We hypothesized that such modifications would block DNA polymerases [47], preventing TUNEL reaction. Finally, DNA did not react to DAPI staining. This response suggests that DNA fragmentation and deterioration were extensive.

During seed ageing, changes in linolenic and linoleic acids serve as sensitive indicators of the lipid oxidation process [58–60]. Oxidation results in a marked decrease in the percentage of linoleic and linolenic acids, to a lesser extent for the latter, as well as in a slight increase in the relative percentage of most saturated fatty acids [61–65]. In this study, we detected significant differences in the profiles of polyunsaturated fatty acids between archeological seeds and controls (Table 1), as follows: (i) a decrease in the relative percentage of polyunsaturated fatty acids; (ii) a relative increase in the percentage of the fractions of saturated fatty acids; and (iii) the presence of the signal (only detected in the archaeological seeds) corresponding to caproic acid (C6:0), which can be attributable to the fragmentation of long-chain fatty acids generated after extensive oxidation. Here, it was possible to infer that the oxidation of fatty acids was associated with the collapse of lipid bodies, as observed by TEM (Fig. 3m–r).

Maillard reactions include spontaneous reactions of reducing sugars with the primary amino groups of proteins and nucleic acids [27]. Non-enzymatic degradation of DNA is initiated by cleavage of the N-glycosidic bond between the sugar backbone and the base; further degradation, through oxidative reactions, leads to excision of the sugar–phosphate backbone, causing single- and double-strand breaks, chemical modification of bases and the crosslinking of carbonyl and amine groups [66]. Maillard reactions perpetuate degradation of DNA fragments into so-called advanced glycosylation endproducts [66]. Such Maillard products have been found in artificially aged quinoa [33] and wheat [67] seeds, among others. In aged quinoa seeds, Castellión et al. [33] demonstrate that protein deterioration, insolubility and Maillard product accumulation are the main causes of viability loss during storage. According to Bernal-Lugo and Leopold [68], protein modification is a process that can occur slowly in dry systems, and might be expected to contribute to dynamic ageing. In dry seeds, protein modification can take place through non-enzymatic glycation with reducing sugars [69] and/or by reacting with α, β-unsaturated aldehydes, which are products of the free radical-mediated oxidation of polyunsaturated fatty acids [70,71]. Also, α, β-unsaturated aldehydes may react with the sulfhydryl groups of proteins to form stable thio-ether derivatives that possess a carbonyl function [72,73]. Here, we were not able to determine how glycation occurred along the time that seeds were stored, but found that, in addition to DNA fragmentation, pro-

teins degraded and glycated, forming Maillard products. Likewise, ageing leads to changes in bean seed coat and browning increases with the duration of ageing, and the reaction of Maillard has been proposed to be responsible for browning [74].

The archaeological embryos here studied exhibited the typical brown color of aged tissues by the Maillard reaction (Fig. 1C). On the other hand, this reaction did not alter the morphology of the protein bodies (Fig. 3j–p), indicating that glycation was an *in situ* reaction. Here, it should be noted that, except for references to some modifications in membranes of human cells, there are no previous reports on changes in cell structures as a consequence of the Maillard reaction.

In summary, it is possible to infer that, at some time during the storage period, a PCD process started and ended. The process led to the reduction of heterochromatin density and total DNA degradation into small fragments (less than 500 bp), as revealed by the ladder analysis, protein glycation and fatty acid oxidation. The process observed is not necrosis because if it were, it would be expected that the fully collapsed heterochromatin had persisted inside the nucleus, and also that the DNA band, as revealed by DNA ladder, had exhibited a size close to that of the control. Even more, necrotic cytological hallmarks include mitochondrial swelling, the absence of growing lytic vacuoles and an early rupture of the plasma membrane [15]. In the cytoplasm of quinoa embryos here studied there are no lytic or non-lytic vacuoles; specifically in the case of the archaeological embryos, similar to that reported in necrosis, dead cells remained barely processed for 2300 years; then, we conclude that death occurred according to a program of PCD probably similar to what occurs in any orthodox seed during seed bank storage.

DNA yield and molecular weight are dependent on the initial condition of the sample and storage conditions that prevent nuclease activity. According to Walters et al. (29), DNA in seeds degrades into small fragments over thousands of years, and the PCR product size in ancient seeds will decrease to less than 300 bp. As an example, the DNA from badly charred seeds is often of higher quality than that from specimens that were morphologically well-preserved [30,31]. It is possible that charred seeds were sterilized by heat, and that the initial and dramatic degradation of DNA at high temperatures may have been balanced in the long term by the inhibition of the PCD process. Hence, specifying whether the death was necrotic or within a PCD is an important issue to define the potential use of DNA for studies of phylogeny or conservation.

Acknowledgment

References

[1] M.E. Tapia, Agrobiodiversidad En Los Andes, Fundación Friederich Ebert, Lima, 1999.
[2] H.D. Bertero, A.J. de la Vega, G. Correa, S.E. Jacobsen, A. Mujica, Genotype and genotype-by-environment interaction effects for grain yield and grain size in quinoa (*Chenopodium quinoa* Willd.) as revealed by pattern analysis of international multi-environment trials, Field Crop. Res. 89 (2004) 299–318.
[3] I. Prego, S. Maldonado, M. Otegui, Seed structure and localization of reserves in *Chenopodium quinoa*, Ann. Bot.-London 82 (1998) 481–488.
[4] M. Gambier, La Cultura De Ansilta, Instituto De Investigaciones Arqueológicas Y Museo, universidad Nacional de San Juan, San Juan, 1977, pp. 1–276.
[5] M. Gambier, La Cultura De Los Morrillos, Instituto De Investigaciones Arqueológicas Y Museo, Universidad Nacional de San Juan, San Juan, 1985, pp. 1–232.
[6] F.A. Roig, Frutos y semillas arqueológicos de Calingasta, San Juan, in: M. Gambier (Ed.), La Cultura De Ansilta, Instituto de Investigaciones Arqueológicas y Museo, Universidad Nacional de San Juan, San Juan, 1977, pp. 215–250.

[7] E.H. Roberts, Predicting the storage life of seeds, Seed Sci. Technol. 1 (1973) 499–514.
[8] M.I. Daws, J. Davies, E. Vaes, R. van Gelder, H.W. Pritchard, Two-hundred year seed survival of Leucospermum and two other woody species from the Cape floristic region, South Africa, Seed Sci. Res. 17 (2007) 73–79.
[9] S. Sallon, E. Solowey, Y. Cohen, R. Korchinsky, M. Egli, I. Woodhatch, O. Simchoni, M. Kislev, Germination, genetics, and growth of an ancient date seed, Science 320 (2008) 1464.
[10] J.M.B. Shen-Miller, J.W. Mudgett, S. Schopf, C.R. Berger, Exceptional seed longevity and robust growth: ancient Sacred Lotus from China, Am. J. Bot. 82 (1995) 1367–1380.
[11] J. Shen-Miller, J.W. Schopf, G. Harbottle, R.J. Cao, S. Ouyang, K.S. Zhou, J.R. Southon, G.H. Liu, Long-living lotus: germination and soil γ-irradiation of centuries-old fruits, and cultivation, growth and phenotypic abnormalities of offspring, Am. J. Bot. 89 (2002) 236–247.
[12] J.M. Farrant, N.W. Pammenter, P. Berjak, C. Walters, Subcellular organization and metabolic activity during the development of seeds that attain different levels of desiccation tolerance, Seed Sci. Res. 7 (1997) 135–144.
[13] N.W. Pammenter, P. Berjak, A review of recalcitrant seed physiology in relation to desiccation-tolerance mechanisms, Seed Sci. Res. 9 (1999) 13–37.
[14] I. Kranner, H. Chen, H.W. Pritchard, S.R. Pearce, S. Birtić, Inter-nucleosomal DNA fragmentation and loss of RNA integrity during seed ageing, Plant Growth Regul. 63 (2011) 63–72.
[15] W.G. Van Doorn, E.P. Beers, J.L. Dangl, V.E. Franklin-Tong, P. Gallois, I. Hara-Nishimura, A.M. Jones, M. Kawai-Yamada, E. Lam, J. Mundy, L.A.J. Mur, M. Petersen, A. Smertenko, M. Taliansky, F. Van Breusegem, T. Wolpert, E. Woltering, B. Zhivotovsky, P.V. Bozhkov, Morphological classification of plant cell deaths, Cell Death Differ. 18 (2011) 1241–1246.
[16] P.V. Bozhkov, L.H. Filonova, M.F. Suárez, Programmed cell death in plant embryogenesis, Curr. Top. Dev. Biol. 67 (2005) 135–179.
[17] P.V. Bozhkov, M.F. Suarez, L.H. Filonova, G. Daniel, A.A. Zamyatnin, S. Rodriguez-Nieto, B. Zhivotovsky, A. Smertenko, Cysteine Protease McII-Pa Executes Programmed Cell Death During Plant Embryogenesis, 102, PNAS, USA, 2005, pp. 14463–14468.
[18] F.J. Domínguez, F.J. Cejudo, Identification of a nuclear-localized nuclease from wheat cells undergoing programmed cell death that is able to trigger DNA fragmentation and apoptotic morphology on nuclei from human cells, Biochem. J. 397 (2006) 529–536.
[19] F.J. Domínguez, F.J. Cejudo, A comparison between nuclear dismantling during plant and animal programmed cell death, Plant Sci. 197 (2012) 114–121.
[20] W. Sakamoto, T. Takami, Nucleases in higher plants and their possible involvement in DNA degradation during leaf senescence, J. Exp. Bot. 65 (2014) 3835–3843.
[21] R. Battelli, L. Lombardi, H.J. Roger, P. Picciarelli, R. Lorenzi, N. Ceccarelli, Changes in ultrastructure, protease and caspase-like activities during flower senescence in Lilium longiflorum, Plant Sci. 180 (2011) 716–725.
[22] M.P. López-Fernández, H.P. Burrieza, A.J. Rizzo, L.J. Martínez-Tosar, S. Maldonado, Cellular and molecular aspects of quinoa leaf senescence, Plant Sci. 238 (2015) 178–187.
[23] G. Rantong, A.H. Gunawardena, Programmed cell death: genes involved in signaling, regulation, and execution in plants and animals, Botany 93 (2015) 193–210.
[24] D.G. Tang, E. La, J. Kern, J.P. Kehrer, Fatty acid oxidation and signaling in apoptosis, Biol. Chem. 383 (2002) 425–442.
[25] S. Tsanko, F. Gechev-Van Breusegem, J.M. Stone, I. Denev, C. Laloi, Reactive oxygen species as signals that modulate plant stress responses and programmed cell death, Bioessays 28 (2006) 1091–1101.
[26] R.G. Lichtenstein, G.A. Rabinovich, Glycobiology of cell death: when glycans and lectins govern cell fate, Cell Death Differ. 20 (2013) 976–986.
[27] F. Van Breusegem, J.F. Dat, Reactive oxygen species in plant cell death, Plant Physiol. 141 (2006) 384–390.
[28] W.G. VanDoorn, E.J. Woltering, Many ways to exit? Cell death categories in plants, Trends Plant Sci. 10 (2005) 117–122.
[29] C. Walters, A.A. Reilley, P.A. Reeves, J. Baszczak, C.M. Richards, The utility of aged seeds in DNA banks, Seed Sc. Res. 16 (2006) 169–178.
[30] P. Goloubinoff, S. Páábo, A.C. Wilson, Evolution of Maize Inferred from Sequence Diversity of an Adh2 Gene Segment from Archaeological Specimens, 90, PNAS, USA, 1993, pp. 1997–2001.
[31] J. Threadgold, T.A. Brown, Degradation of DNA in artificially charred wheat seeds, J. Arch. Sci. 30 (2003) 1067–1076.
[32] R.H. Ellis, T.D. Hong, E.H. Roberts, A low moisture-content limit to logarithmic relation between seed moisture content and longevity, Ann. Bot.-London 61 (1988) 405–408.
[33] M. Castellión, S. Matiacevich, M.P. Buera, S. Maldonado, Protein deterioration and longevity of quinoa seeds during long-term storage, Food Chem. 121 (2010) 952–958.
[34] M. Castellión, S. Maldonado, M.P. Buera, Molecular mobility and seed longevity in Chenopodium quinoa, in: D.S. Reid, T. Sajjaanantakul, P.J. Lillford, S. Charoenrein (Eds.), Water Properties in Food, Health, Pharmaceutical and Biological Systems: ISOPOW 10, Wiley-Blackwell, Oxford, 2010, pp. 647–656.
[35] K.F. Harris, Z. Pesic-Van Esbroeck, J.E. Duffus, Moderate-temperature polymerization of LR White in a nitrogen atmosphere, Microsc. Res.Tech. 32 (1995) 264–265.
[36] F. Otto, DAPI staining of fixed cells for high-resolution flow cytometry of nuclear DNA, Methods Cell Biol. 33 (1990) 105–110.
[37] C. Riccardi, I. Nicoletti, Analysis of apoptosis by propidium iodide staining and flow cytometry, Nat. Protoc. 1 (2006) 1458–1461.
[38] D.J. Thornton, I. Carlsteldt, J.K. Sheehan, Identification of glycoproteins on nitrocellulose membranes and gels, Mol. Biotechnol. (1996) 171–176.
[39] E.G. Bligh, W.J. Dyer, A rapid method of total lipid extraction and purification, Can. J. Biochem. Physiol. 37 (1959) 911–917.
[40] G. Nicoletti, M.C. Migliorati, F. Pagliacci, C. Grignani, Riccardi, A rapid and simple method for measuring thymocyte apoptosis by propidium iodide staining and flow cytometry, J. Immunol. Methods 139 (1991) 271–279.
[41] D.J. Wright, The seed globulins, in: B.J.F. Hudson (Ed.), Development in Food Proteins, Elsevier Applied Science, London, 1987, pp. 81–157.
[42] C. Brinegar, S. Goundan, Isolation and characterization of chenopodin, the 11S seed storage protein of quinoa (Chenopodium quinoa), J. Agr. Food Chem. 41 (1993) 182–185.
[43] D.J. Fairbanks, K.W. Burgener, L.R. Robison, W.R. Andersen, E. Ballon, Electrophoretic characterization of quinoa seed proteins, Plant Breeding 104 (2006) 190–195.
[44] G.D. Zazula, C.-R. Harington, A.M. Telka, F. Brock, Radiocarbon dates reveal that Lupinus arcticus plants were grown from modern not Pleistocene seeds, New Phytol. 182 (2009) 788–792.
[45] A.E. Porsild, C.R. Harington, G.A. Mulligan, Lupinus arcticus Wats. grown from seeds of Pleistocene age, Science 158 (1967) 113–114.
[46] S.G. Yashina, S.V. Gubin, E.V. Shabaeva, E.F. Egorova, S.V. Maksimovich, Viability of higher plant seeds of Late Pleistocene age from permafrost deposits as determined by in vitro culturing, Dokl. Biol. Sci. 282 (2002) 151–154.
[47] W.C. Earnshaw, Nuclear changes in apoptosis, Curr. Opin. Cell Biol. 7 (1995) 337–343.
[48] M.T.P. Gilbert, E. Willerslev, A.J. Hansen, I. Barnes, L. Rudbeck, N. Lynnerup, A. Cooper, Distribution patterns of post-mortem damage in human mitochondrial DNA, Am. J. Hum. Genet. 72 (2003) 32–47.
[49] M.T.P. Gilbert, E. Willerslev, A.J. Hansen, I. Barnes, L. Rudbeck, N. Lynnerup, A. Cooper, Characterisation of genetic miscoding lesions caused by post-mortem damage, Am. J. Hum. Genet. 72 (2003) 48–61.
[50] S. Pääbo, R.G. Higuchi, A.C. Wilson, Ancient DNA and the polymerase chain reaction. The emerging field of molecular archaeology, Biol. Chem. 264 (1989) 9709–9712.
[51] T. Lindahl, Instability and decay of the primary structure of DNA, Nature 362 (1993) 709–715.
[52] O. Handt, M. Höss, S. Pääbo, D.N.A. Ancient, (methodological challenges), Experientia 50 (1994) 524–529.
[53] M. Höss, P. Jaruga, T.H. Zastawny, M. Dizdaroglu, DNA damage and DNA sequence retrieval from ancient tissues, Nucleic Acids Res. 24 (1996) 1304–1307.
[54] N. Bastos Lima, F. Gomes Trindade, M. Da Cunha, A.E. Amancio Oliveira, J. Tping, K. Lindsey, K. Valevski Sales Fernandes, Programmed cell death during development of cowpea (Vigna unguiculata (L.) Walp.) seed coat, Plant Cell Environ. 38 (2015) 716–728.
[55] H. Swift, The constancy of desoxyribose nucleic acid in plant nuclei, Proc. Natl. Acad. Sci. U. S. A. 36 (1950) 643–654.
[56] M. Pfosser, Z. Magyar, L. Bögre, Cell cycle analysis in plants, in: J. Doležel, J. Greilhuber, J. Suda (Eds.), Flow Cytometry with Plant Cells. Analysis of Genes, Chromosomes and Genome, WILEY-VCH Verlag GmbH and Co. KGaA, Weinheim, 2007, pp. 323–348.
[57] A. Bertho, M.A. Santiago, S.G. Coutinho, Flow Cytometry in the Study of Cell Death, 95, Memórias do Instituto Oswaldo Cruz, 2000, pp. 429–433.
[58] D.O. Wilson, M.B. McDonald, The lipid peroxidation model of seed ageing, Seed Sci.Technol. 14 (1986) 269–300.
[59] G. Roqueiro, S. Maldonado, M.C. Ríos, H. Maroder, Fluctuation of oxidative stress indicators in Salix nigra seeds during priming, J. Exp. Bot. 63 (2012) 3631–3642.
[60] L. Colville, E.L. Bradley, A.S. Lloyd, H.W. Pritchard, L. Castle, I. Kranner, Volatile fingerprints of seeds of four species indicate the involvement of alcoholic fermentation, lipid peroxidation, and Maillard reactions in seed deterioration during ageing and desiccation stress, J.Exp. Bot. 63 (2012) 6519–6530.
[61] R. Kalpana, K.V.M. Rao, Lipid changes during accelerated ageing of seeds of pigeonpea (Cajanus cajan (L) Millsp) cultivars, Seed Sci. Technol. 24 (1996) 475–483.
[62] M.T. Aiazzi, J.A. Arguello, A. Pérez, J. DiRienzo, C.A. Guzmán, Deterioration in Atriplex cordobensis (Gandoger et Stuckert) seeds: natural and accelerated ageing, Seed Sci. Technol. 25 (1997) 147–155.
[63] C. Bailly, A. Benamar, F. Corbineau, D. Come, Free radical scavenging as affected by accelerated ageing and subsequent priming in sunflower seeds, Physiol. Plant. 104 (1998) 646–652.
[64] A. Goel, I.S. Sheoran, Lipid peroxidation and peroxide scavenging enzymes in cotton seeds under natural ageing, Biol. Plant. 46 (2003) 429–434.
[65] P. Tammela, M. Nygren, I. Laasko, A. Hopia, H. Vuorela, R. Hiltunen, Volatile compound analysis of ageing Pinus sylvestris L. (Scots pine) seeds, Flavour Frag. J. 18 (2003) 290–295.
[66] A.B. Britt, DNA damage and repair in plants, Annu. Rev. Plant Physiol. Plant Mol. Biol. 47 (1996) 75–100.
[67] I. Strelec, Z. Ugarcic-Hardi, M. Hlevnjak, Accumulation of Amadori and Maillard products in wheat seeds aged under different storage conditions, Croat. Chem. Acta 8 (2008) 131–137.
[68] I. Bernal-Lugo, A. Leopold, The dynamics of seed mortality, J. Exp. Bot. (1998) 1455–1461.

[69] W.Q. Sun, A.C. Leopold, The Maillard reaction and oxidative stress during ageing of soybean seeds, Physiol. Plant. 94 (1995) 94–104.

[70] D.A. Priestley, A.C. Leopold, Lipid changes during natural ageing of soybeans, Physiol. Plant. 59 (1983) 467–470.

[71] D.A. Priestley, B.G. Warner, A.C. Leopold, M.B. McBride, Organic free radical levels in seeds and pollen, Physiol. Plant. 64 (1985) 88.

[72] E. Stadtman, Protein oxidation and ageing, Science 257 (1992) 1220–1224.

[73] M.B. Mudgett, S. Clark, Characterization of plant l-isoaspartylmethyltransferases that may be involved in seed survival: purification, cloning and sequence analysis of the wheat germ enzyme, Biochemistry 32 (1993) 11100–11111.

[74] A.G. Taylor, T.G. Min, D.H. Paine, Maillard reaction causes browning in bean seed coat during ageing: inhibition by aminoguanidine, in: M. Black, K.J. Bradford, J. Vazquez-Ramos (Eds.), Seed Biology Advances and Applications, CAB International, Wallingford, 2000, pp. 189–196.